A PHOTOGRAPHIC INVESTIGATION OF BUBBLE NUCLEATION FROM ARTIFICIAL CAVITIES

by

John Christian Eller

UNITED STATES
NAVAL POSTGRADUATE SCHOOL

THESIS

A PHOTOGRAPHIC INVESTIGATION OF BUBBLE

NUCLEATION FROM ARTIFICIAL CAVITIES

by

John Christian Eller

June 1968

Technical Reports Collection

Citation Format: Full Citation (1F)

Accession Number :
AD0849776
Citation Status:
Active
Citation Classification:
Unclassified
Field(s) & Group(s):
070400 - PHYSICAL CHEMISTRY
140400 - PHOTOGRAPHY
Corporate Author:
NAVAL POSTGRADUATE SCHOOL MONTEREY CA
Unclassified Title:
A Photographic Investigation of Bubble Nucleation from Artificial Cavities.
Title Classification:
Unclassified
Descriptive Note:
Master's thesis,
Personal Author(s):
Eller, John Christian
Report Date:
01 Jun 1968
Media Count:
53 Page(s)
Cost:
$7.00
Report Classification:
Unclassified
Descriptors:
(*NUCLEATE BOILING, , HIGH SPEED PHOTOGRAPHY), MOTION PICTURE PHOTOGRAPHY, BUBBLES, WATER, ETHANOLS, INTERFACES, THESES
Abstract:
High speed motion pictures of bubble nucleation from glass capillaries were obtained. The fluids used were: distilled water, water with wetting agent, water with sucrose, and ethanol. Capillaries of cylindrical, conical, and reentrant geometries were used with inner diameters ranging from .0182 to .0381 inches. The penetration of the liquid-vapor interface into a cavity after bubble departure appeared to be inertia controlled. Cavity interior geometry and cleanliness had a direct effect upon the liquid-vapor interface penetration distance. The depth of penetration of the interface increased as cavity size increased. Viscosity reduced the interface penetration. Bubble growth curves were obtained for a typical bubble in each fluid. Bubble departure diameter appeared to be independent of cavity geometry but increased as cavity size increased. Viscosity retarded bubble growth during the initial stages of growth. (Author)
Abstract Classification:
Unclassified
Distribution Limitation(s):
01 - APPROVED FOR PUBLIC RELEASE

Source Code:
251450
Document Location:
DTIC
Change Authority:
ST-A USNPS LTR, 1 OCT 71

A PHOTOGRAPHIC INVESTIGATION OF BUBBLE NUCLEATION FROM ARTIFICIAL CAVITIES

by

John Christian Eller
Lieutenant, United States Navy
B.S., United States Naval Academy, 1962

[redacted]

Submitted in partial fulfillment of the
requirements for the degree of

MASTER OF SCIENCE IN MECHANICAL ENGINEERING

from the

NAVAL POSTGRADUATE SCHOOL
June 1968

ABSTRACT

High speed motion pictures of bubble nucleation from glass capillaries were obtained. The fluids used were: distilled water, water with wetting agent, water with sucrose, and ethanol. Capillaries of cylindrical, conical, and reentrant geometries were used with inner diameters ranging from .0182 to .0381 inches.

The penetration of the liquid-vapor interface into a cavity after bubble departure appeared to be inertia controlled. Cavity interior geometry and cleanliness had a direct effect upon the liquid-vapor interface penetration distance. The depth of penetration of the interface increased as cavity size increased. Viscosity reduced the interface penetration.

Bubble growth curves were obtained for a typical bubble in each fluid. Bubble departure diameter appeared to be independent of cavity geometry but increased as cavity size increased. Viscosity retarded bubble growth during the initial stages of growth.

TABLE OF CONTENTS

LIST OF TABLES

LIST OF FIGURES

LIST OF FIGURES (Contd.)

LIST OF SYMBOLS

SYMBOL	DEFINITION
D	Bubble diameter, in.
f	Bubble frequency, sec^{-1}
L	Cavity depth, in.
t	Time, sec.
T	Bubble period, sec.
T	Temperature (used with subscripts), deg F
x*	Maximum penetration distance of the liquid-vapor interface inside a cavity, in.
R	Radius of curvature of the liquid-vapor interface, in.
σ	Surface tension, dynes/cm
θ	Contact angle of the liquid-vapor interface with the cavity walls, deg.
γ	Surface energy, dynes/cm

Subscripts

d	Departure
v	Vapor
m	Bulk mean
sat	Saturation at atmospheric pressure
sv	Solid-vapor interface
sl	Solid-liquid interface
lv	Liquid-vapor interface
g	Growth

ACKNOWLEDGEMENTS

The author wishes to express his gratitude to Dr. Paul Marto of the Naval Postgraduate School for his generous contributions of time, constructive criticism, encouragement and patience.

The author is deeply grateful to Mrs. Eller for her understanding and support during the pursuit of this work.

1. INTRODUCTION

1.1 Background

The nucleate boiling regime is of great interest because of the efficient manner in which large quantities of heat can be removed from a relatively small surface. During nucleate boiling, it is generally agreed that bubbles form (nucleation) at definite sites on solid surfaces. As Rohsenow [1] points out in his excellent survey of boiling heat transfer, the exact nature of these nucleation sites or "nuclei" remains a mystery, but these sites probably are tiny imperfections in the form of pits and scratches on the boiling surface. The basic question with nucleate boiling is why some "nuclei" are proficient at causing nucleation and others are not. Westwater [2] summarizes some of the beliefs concerning nucleation sites by stating that in order for a site to nucleate, it must contain trapped vapor (or gas) when the container in which the site is located is filled with fluid. The size and shape of the imperfections determine whether or not vapor (or gas) can be trapped and also how much liquid superheat is necessary for nucleation to occur.

Marto and Rohsenow [3] developed a model for bubble nucleation in alkali metals. They derived an expression for the maximum penetration distance, x^*, of the liquid-vapor interface into a cavity after a bubble departs. This penetration distance is dependent upon several variables: fluid properties (density, surface tension, specific heat, heat of vaporization, thermal conductivity), heat flux, surface material properties (thermal diffusivity, thermal conductivity, density, specific heat), and cavity geometry (cavity depth, cavity radius). The penetration distance, x^*, may be used as a measure of the stability of a cavity. A cavity is defined as being stable if it does not fill up with liquid (deactivate)

once it has begun to nucleate bubbles. Cavity geometry is important since x* is inversely proportional to cavity depth, L, and radius of curvature, R. If R increases with increasing penetration depth as in a reentrant cavity, stability should improve. Conversely, if the radius of curvature decreases with increasing penetration depth as in a conical cavity, then stability should be decreased. This is shown schematically in Fig. 1.

The theory of Marto and Rohsenow postulates for nucleate boiling of liquid alkali metals that after a bubble has departed, liquid rushes down into the cavity mouth. They predict that the liquid-vapor interface will recede into the cavity until the bulk liquid and vapor temperatures are equal. At this point, interface motion stops and the bubbles begin to grow. DuBois [4] found that the model of Marto and Rohsenow did not adequately describe the mechanism of boiling for the fluids used in his work. He observed that, while boiling with ethanol and liquid nitrogen, penetration took place before bubble departure. DuBois did observe however, that interface penetration appeared to be inversely proportional to cavity radius of curvature. DuBois was unable to obtain interface penetration data for distilled water, water with wetting agent or water with sucrose mixture to test further the validity of the Marto and Rohsenow model.

Although the model developed by Marto and Rohsenow is not completely adequate for boiling non-metals, the variables which affect stability (fluid properties, material properties, heat flux and cavity geometry) are pertinent for cavities during boiling in any fluid.

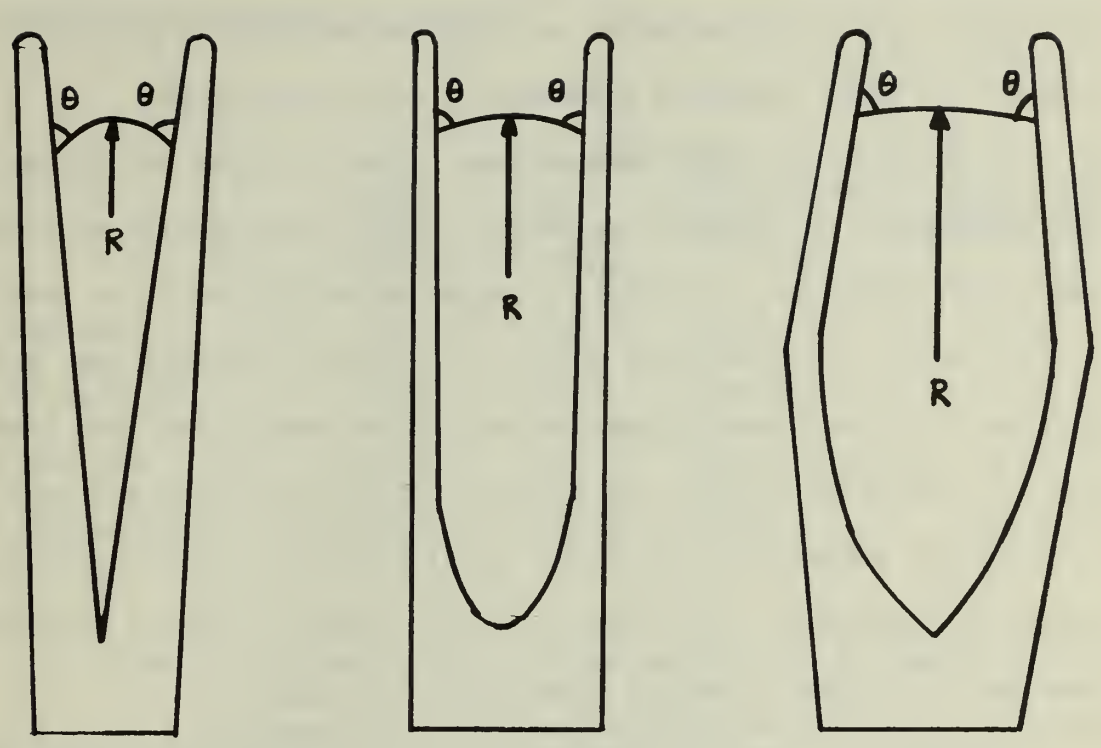

Conical Cylindrical Reentrant

$R_{Reentrant} > R_{Cylindrical} > R_{Conical}$

For Same Inner Diameter and Meniscus Contact Angle, θ

FIG. 1

Schematic Diagram of Cavity Geometry and Radius of Curvature Relationships

Thesis Objective

1.2 The objective of this thesis was to gain additional information concerning the boiling mechanism. In particular, the effect of fluid properties, and cavity geometry on interface penetration and bubble growth from glass capillary tubes was of prime importance.

In addition, in order to study the effect of fluid properties and cavity geometry on interface penetration while boiling with water and water with additives, a detailed cleaning procedure was to be developed.

In order to achieve this objective, cavities with the same geometry but different inner diameters were to be constructed from pyrex tubing. It was realized that the cavities would not present an ideal model of a typical nucleation site since the size would be much larger than normal imperfections. The cavities would, however, offer a good model from which to study interface penetration and motion.

Finally, as a means of analyzing in detail the boiling mechanism, high speed motion pictures were to be taken.

2. DESCRIPTION OF EXPERIMENTAL EQUIPMENT AND PROCEDURES

2.1 Equipment.

Four artificial cavities were constructed from Pyrex tubing with dimensions tabulated in Table I.

TABLE I

SHAPE	CAVITY GEOMETRIES			
	MOUTH O.D. INCHES	MOUTH I.D. INCHES	CAVITY DEPTH INCHES	CAVITY DEPTH / CAVITY I.D.
Conical	.0579	.0381	.1318	3.46
Cylindrical	.0595	.0380	.2728	7.18
Reentrant	.0582	.0379	.2909	7.67
Cylindrical	.0288	.0182	.1865	10.25

A two inch diameter Pyrex boiler as employed by DuBois [4] with a flat two inch diameter window located just above the base, was used for all experimental runs. A rubber stopper was used to seal the top of the boiler and to mount the artificial cavities. Vapors were condensed with a refluxing condenser using cold tap water. Each cavity was attached to the sealed end of a Pyrex tube and the tube then bent into the form of a "J".

Heat was supplied to the boiler from a Bunsen burner so that the heat flux could be varied rapidly. The boiler rested on a wire mesh screen and was supported by a clamp to the condenser. Figure 2 shows the boiler with condenser installed.

Temperature measurements were accomplished by using two 40 gauge copper-constantan thermocouples mounted in small Pyrex tubes which could be raised and lowered in the boiler. In addition, one of the thermocouples could be rotated in an arc to observe temperature at various

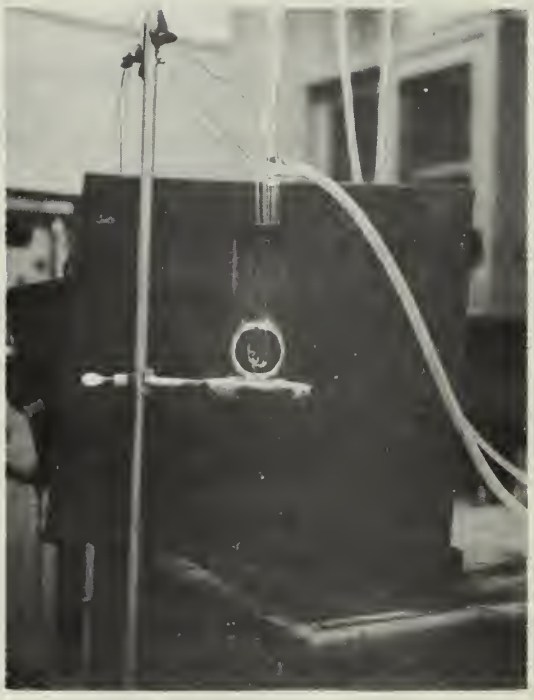

FIG. 2

Photograph of Boiler with Cavities Mounted

locations in proximity to the cavities. The thermocouples were wired through a single selector switch box which was bucked against an ice junction. The generated EMF was read on a Leeds and Northrup K-3 Universal Potentiometer using a null meter.

High speed motion pictures were taken using a Fairchild Model H S 401 Motion Analysis Camera capable of film speeds up to 8000 frames per second. Four hundred foot rolls of 16mm Eastman Kodak Tri-X film were used for all experimental runs. The camera was mounted on a Fairchild Model H S 2511 tripod so that the camera could be raised or lowered while focusing. A Fairchild Model H S 10600 Timing Light Generator, capable of 1000 cycles per second, was used to place timing marks on the film.

Power was supplied to the camera by a Fairchild Model H S-5101B D. C. Power Supply capable of producing 60 volts with 30 amps of current.

The optical portion of a Gaertner optical strain gauge readout system was used for the camera lens system. This lens gave a magnification of 20x.

Lighting was supplied by a Colortran Quality-King 500 Light Fixture with a G. E. PAR-64 1000 watt quartz iodine spotlight and glass heat shield. The light was positioned 15 inches behind the boiler so that it would shine directly into the camera lens. Figure 3 shows a photograph of the experimental setup.

The film was processed in a Fairchild Mini Rapid Film Processor using commercially purchased chemicals as directed by the manufacturer. An ion exchange column and mechanical filter were used with the water wash in an attempt to reduce water marking on the soft emulsion film.

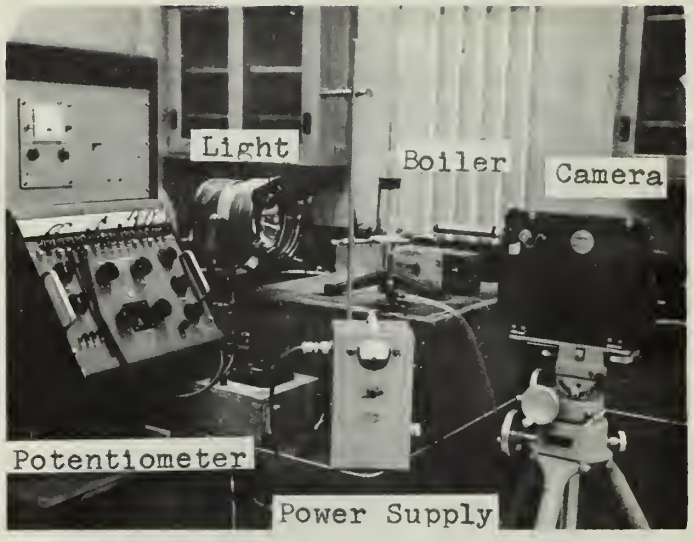

FIG. 3

Photograph of Experimental Apparatus

2.2 Experimental Procedures

The boiler was cleaned before each run in an ultrasonic cleaner for 30 minutes using commercial alkaline powder and water solution as a cleanser. The boiler was then filled with chromic-sulphuric acid cleaning solution and allowed to heat for one hour. The cleaning solution was made with Chromerge, a commercially available solution, and sulphuric acid. Finally, the boiler was rinsed in a distilled water bath and then filled with the test fluid to a fixed level which was the same for all runs.

A detailed cleaning procedure was followed in cleaning the interior of the cavities in an attempt to observe interface penetration during boiling. The cavities were filled with the chromic-sulphuric acid solution and then inserted in a hot acid bath of the same solution and allowed to sit for one hour. The acid was then extracted from the cavities, and the cavities were flushed with distilled water. A hypodermic needle, which was also acid cleaned before each use, was employed in inserting and removing the acid and distilled water. After cleaning and before mounting in the rubber stopper, each cavity was set in a covered container in an attempt to reduce the exposure of the cavities to air currents. The cavities were immediately mounted in the rubber stopper and inserted in the filled boiler.

During the early stages of the experimental work, an attempt was made to boil with all four cavities simultaneously; however, with this procedure, interface penetration was not observed with distilled water. The length of time to mount a cavity in the stopper was on the order of three times longer than the time it took to clean it. Therefore, the poor results obtained while boiling with four cavities was postulated to

be due to the long time of exposure to the atmosphere and thus contamination of the cavity interior. In order to reduce the exposure time, only two cavities were cleaned and employed in each data run.

After insertion of the cavities into the boiler, heat was applied to the boiler and the cooling water to the condenser was turned on. The fluid was allowed to heat and boil for 30 minutes. The temperature of the vapor immediately above the fluid surface and the temperature of the fluid in the vicinity of the cavities were recorded for determining the mean fluid temperature, T_m and the saturation temperature, T_{sat}. The light was then turned on and the camera run. The camera would vibrate while running since the mounting fixtures on the tripod were not completely rigid.

Focusing of the camera was accomplished as follows. Marks were made on the loaded film with a felt tip marker. The marked frame was then positioned opposite a bore sight view finder attached to the camera. The light was turned on and the camera was prefocused on the marked film by adjusting the bore sight view finder. The camera was adjusted to achieve the clearest image of the cavities in the boiler. The bore sight view finder was removed prior to running the camera.

Four fluids were used: distilled water, water with wetting agent, water with viscous agent (sucrose), and ethanol. The addition of .04 weight per cent of cetyltrimethylammonium bromide (a conventional wetting agent) to water decreases its surface tension at 25°C from 71.9 dynes/cm to 32 dynes/cm as pointed out by DuBois [4]. This fluid was used to study the effects of reduced surface tension.

The effects of a viscous agent were studied using a 60 weight per cent solution of sucrose and distilled water. As determined by DuBois [4], this fluid has a viscosity of 291.5 millipoise compared with 8.937

millipoise of ordinary water at 25°C.

Six data taking runs were made using various fluids and cavity geometries. These runs are summarized in Table II. The procedure was the same for all runs with the exception of the two ethanol runs. With ethanol, when vigorous boiling began, the conical cavity deactivated after approximately fifteen seconds and the cylindrical cavities deactivated after approximately forty-five seconds. Therefore, photographic pictures were taken in these two runs immediately after boiling commenced.

For each run the following data was taken:

a) interface penetration

b) contact angle with inside surface of cavity

c) growth data

d) bubble departure diameter

2.3 Measurement Techniques in Analyzing Films

Each film was analyzed by projecting it from a standard 16mm movie screen onto a ground glass screen. An analyzer was used to advance the film either continuously or frame by frame.

Dimensions of each cavity were obtained using dividers and were measured on an engineer's scale of sixty divisions per inch. The outer diameter of the cavities was measured by a micrometer with accuracy of $\pm$ .0001 inches. The engineer's scale could be read to $\pm$ .5 divisions giving an accuracy for a typical scale factor of .000793 $\pm$ .000005 inches per division. Bubble diameter was measured from the movie screen using the dividers and engineer's scale. The smallest distance measured was on the order of .003 inches. Therefore the accuracy of the diameter measurements was $\pm$ .0004 inches. This introduced a maximum error of

TABLE II

SUMMARY OF EXPERIMENTAL RUNS

RUN NUMBER	CAVITY GEOMETRY	FLUID
5	Conical Cylindrical	distilled water
6	Reentrant Small Cylindrical	distilled water
7	Conical Cylindrical	distilled water & .04wt. % wetting agent
8	Conical Cylindrical	60% sucrose solution
10	Reentrant Small Cylindrical	ethanol
11	Conical Cylindrical	ethanol

16% in diameter measurements.

Interface penetration was measured as the distance from top of the cavity to the maximum depth at which the liquid-vapor interface meniscus was in contact with the cavity wall. The smallest interface penetration distance was approximately .001 inches. With an accuracy in measurement of $\pm$ .0004 inches, a maximum error of 40% is introduced into interface penetration measurement.

Bubble size was determined in the following manner. During early stages of growth, before the bubble reached a spherical shape, bubble diameter was measured as the height above the top of the cavity. When the bubble became spherical the diameter was measured as the horizontal diameter. During the final stages of growth, when the bubble severely elongated, the diameter was again measured as the horizontal diameter. Departure diameter was measured as the average of vertical and horizontal distances.

The angle that the liquid-vapor interface makes with the cavity walls is the contact angle, θ. This was measured by placing a protractor with sliding arm on the glass movie screen and measuring the angle from the image. Due to the inaccuracies inherent in trying to determine the exact slope of the interface at the cavity wall, the accuracy of the contact angle measurement is approximately $\pm$ 10°. A schematic for measurement of interface penetration distance, x^*, and contact angle, θ is given on page 24.

Time measurements were obtained by counting marks placed on the film by a timing light generator. The accuracy of time measurements was considered exact.

Bubble growth period, T, is the time between bubble departures and

the bubble frequency is $f = \frac{1}{T}$. These values were obtained from timing marks on the film.

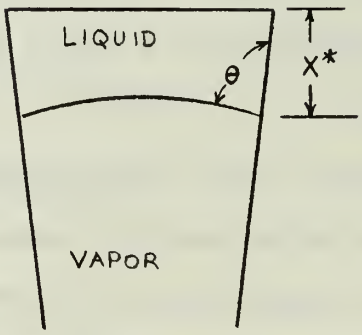

3. PRESENTATION OF DATA AND DISCUSSION

The data is presented in several subsections and consists of film strips showing bubble nucleation, interface penetration data, growth curves and departure diameters.

3.1 Photographic Data and Penetration Distances.

The photographic data is presented in the form of film strips. In the film strips, the cavities are shown at the bottom with the bubble departure at the top. The bottom of the cavities are not shown since the field of view had to be raised in order to photograph the departing bubble.

3.1.1 Boiling Water.

Figure 4 is a series of photographs showing bubble departure and interface penetration for conical, cylindrical, reentrant, and small cylindrical cavities in water. Notice that all cavities show interface penetration after the bubble has departed. The theory of Marto and Rohsenow predicts that as radius of curvature, R, is increased, the penetration distance will decrease. Table III, a tabulation of penetration distances, demonstrates this. For the same inner diameter, the greatest penetration occurs in the conical cavity, the least in the reentrant cavity and an intermediate value in the large cylindrical cavity. The small cylindrical cavity has the least penetration of the four cavities. Cavity depth may also be an important factor here. Since Marto and Rohsenow predict that penetration is inversely proportional to cavity depth, L, then as the ratio of L/D increases, cavity stability should improve. This is the trend observed in this experimental work (See Table 1). However, the radius of curvature appears to be a more important variable on stability than cavity depth since DuBois [4]

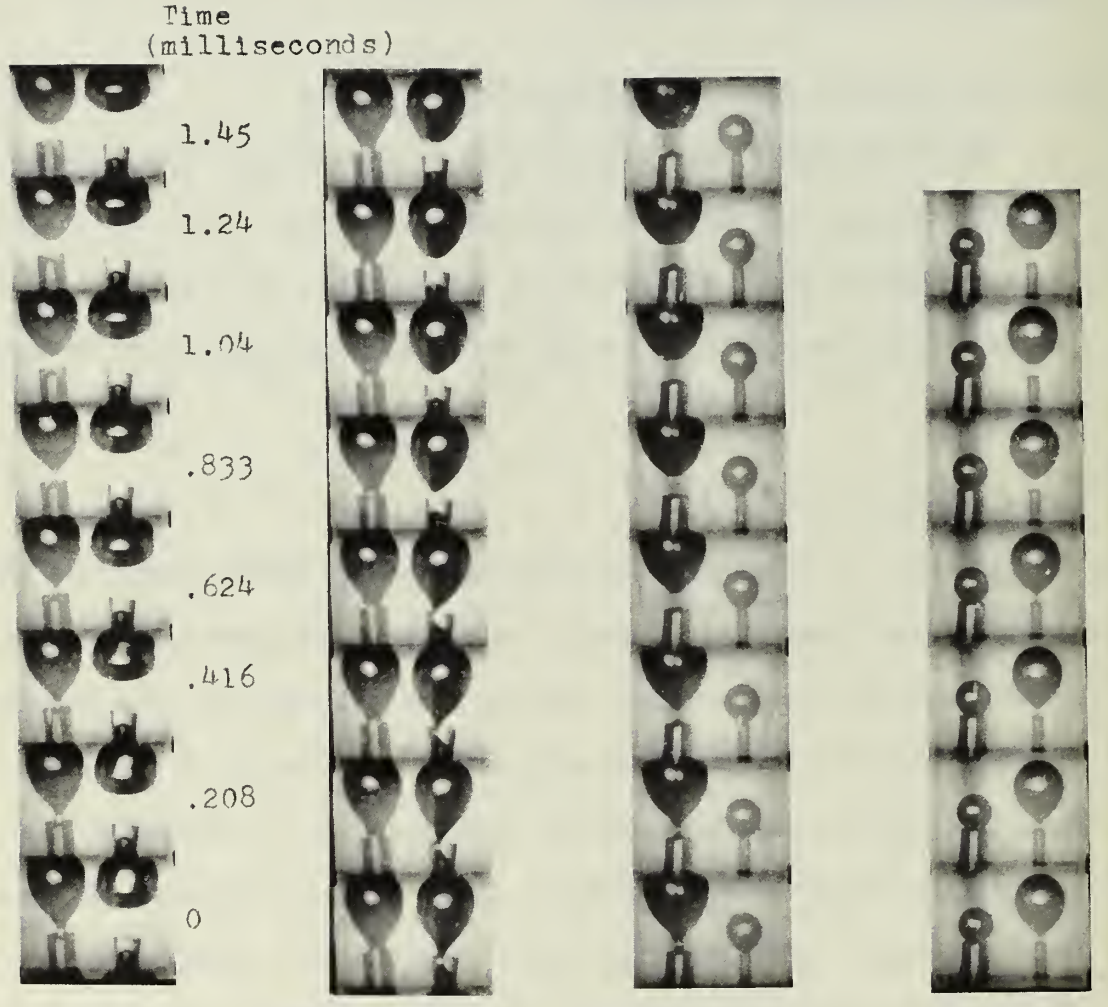

Film Speed 4800 fps

FIG. 4

Photographs of
Bubble Departure and Interface Motion for Cylindrical, Conical, Reentrant and Small Cylindrical Cavities Boiling in Water

TABLE III

PENETRATION DISTANCES IN GLASS CAVITIES FOR VARIOUS FLUIDS AND GEOMETRIES

FLUID	GEOMETRY		X* (in.)
water	conical	same I.D.	.0339
	cylindrical	same I.D.	.0146
	reentrant	same I.D.	.0024
	small cylindrical		.0008
water with wetting agent	conical	same I.D.	.0161
	cylindrical	same I.D.	.0064
water with sucrose	conical	same I.D.	.0161
	cylindrical	same I.D.	.0136
ethanol	conical	same I.D.	.0177
	cylindrical	same I.D.	.0251
	reentrant	same I.D.	.0181
	small cylindrical		.0106

observed that with the ratio of L/D constant, penetration distance decreased as radius of curvature increased. Since the small cylindrical cavity has the least penetration of all four cavities then it appears that small diameter cavities are more stable when compared with larger cavities of any geometry.

In the sequence of photographs for the conical cavity, note the inrush of fluid and extreme necking down of the bubble on one side of the cavity. This unsymmetrical necking down may be due to attraction from the adjacent bubble growing from the cylindrical cavity but more probably it is due to gravity forces since the cavity was slightly tilted. The theory of Marto and Rohsenow predicts that liquid rushes into the cavity only after bubble departure. In their analysis, they neglected the effect of inertia forces on interface motion. It may be, however, that inertia forces cause the observable inrush of fluid while the bubble is necking down.

In an effort to determine what the boiling mechanism is for fluids used in this experimental work, Figs. 5(a), 5(b), 6, 7, 8(a) and 8(b) were drawn. These figures show bubble profiles before and after bubble departure for the conical cavity in each fluid. These were drawn to illustrate the effect of fluid properties on the contact angle θ, on the necking down process and on the motion of the liquid-vapor interface after bubble departure. Figure 5(a) shows the bubble growing and the asymmetrical necking down in the water. The shape of the interface is also shown immediately after bubble departure. Notice that even though the interface is not symmetric, the contact angle with the cavity walls is constant. Figure 5(b) shows slight interface motion after bubble departure which is probably due to oscillations of the top of the interface and an attempt of the interface to become symmetric in the cavity.

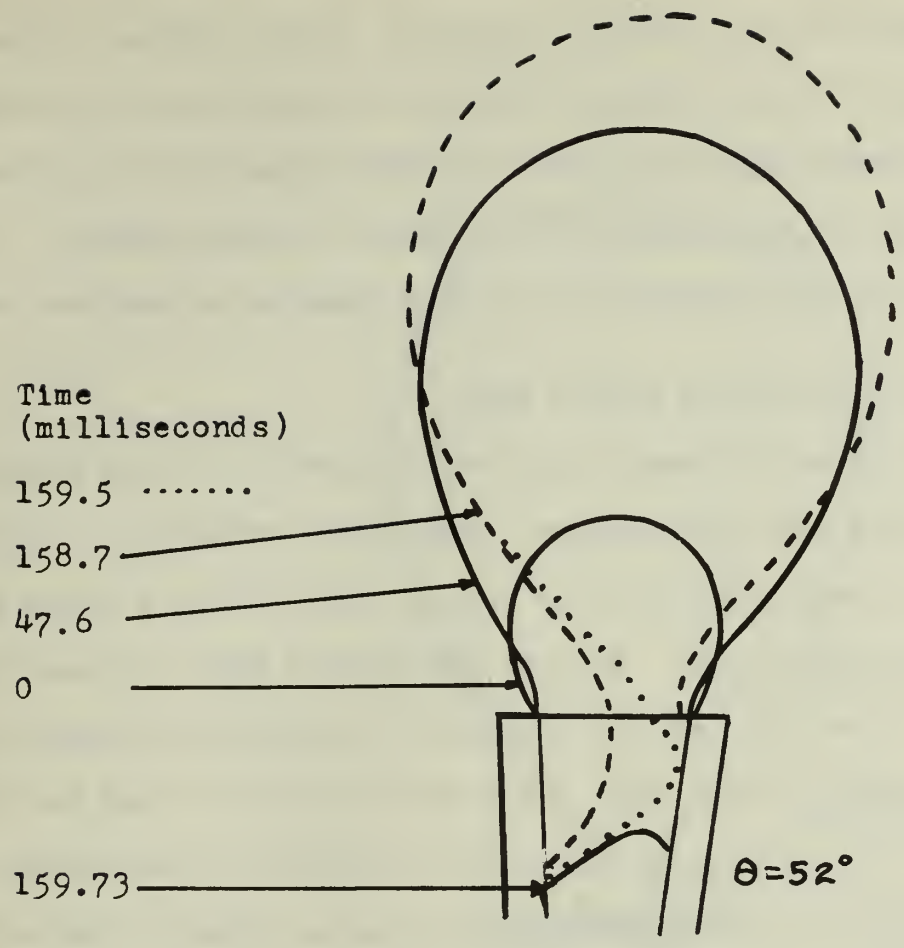

FIG. 5(a)

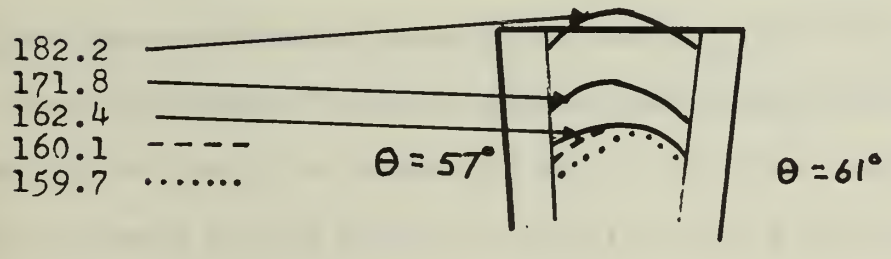

FIG. 5(b)

Bubble and Liquid-Vapor Interface Profiles for Large Conical Cavity in Water

Surface tension forces probably cause this. It was noticed in these figures for all of the working fluids that the liquid-vapor interface was at the maximum penetration when the bubble departed. Any motion of the interface was oscillation and an attempt to become symmetric. This is contrary to the prediction of Marto and Rohsenow as mentioned earlier.

3.1.2 Boiling Water With Wetting Agent.

Figure 9 shows cylindrical and conical cavities boiling simultaneously in water with wetting agent. Notice the asymmetrical necking down which is very apparent in the conical cavity and to a lesser extent in the cylindrical cavity. The data tabulated in Table III again demonstrates the effect of radius of curvature on penetration distance. As can be seen, the conical cavity has greater penetration than the cylindrical cavity. It was expected that with the addition of the wetting agent to distilled water, more penetration would occur. However, Table III shows the penetration to be less for the cavities in water with wetting agent. Figure 6 shows the shape of the bubble while necking down and the liquid-vapor interface after departure. The contact angle with the cavity walls is constant and essentially the same as for water (see Fig. 5(a)). Since the angle θ is a useful inverse measure of wettability, it appears from this data that the addition of the wetting agent has little effect on the wetting characteristics of water. Zisman [5] points out that the contact angle of a liquid is treated as a result of the mechanical equilibrium of a drop of liquid on a solid surface under the action of three surface tensions or surface energies (See the figure page 35): γ_{LV} at the interface of the liquid and vapor phases, γ_{SV} at the interface of the solid and vapor, and γ_{SL} at the interface of the solid and liquid.

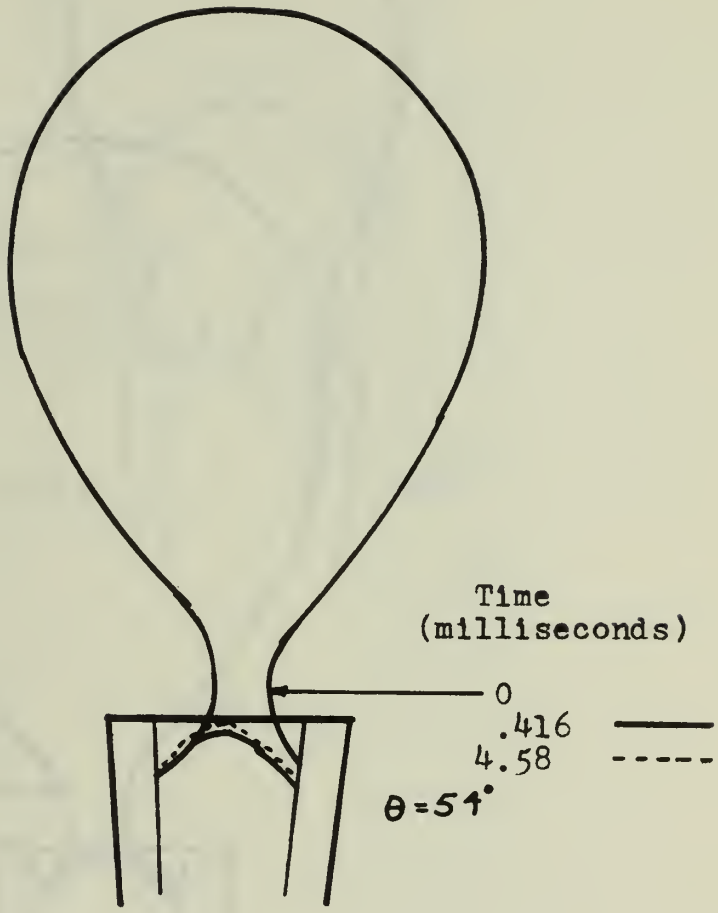

FIG. 6

Bubble and Liquid-Vapor Interface Profiles for Large Conical Cavity in Water with Wetting Agent

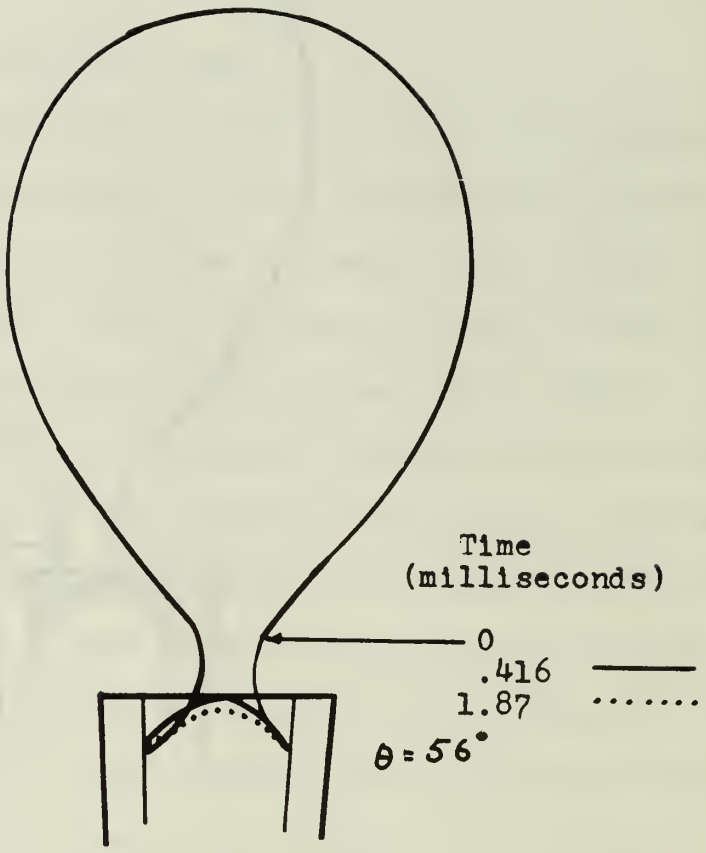

FIG. 7

Bubble and Liquid-Vapor Interface Profiles for Large Conical Cavity in Water with Sucrose

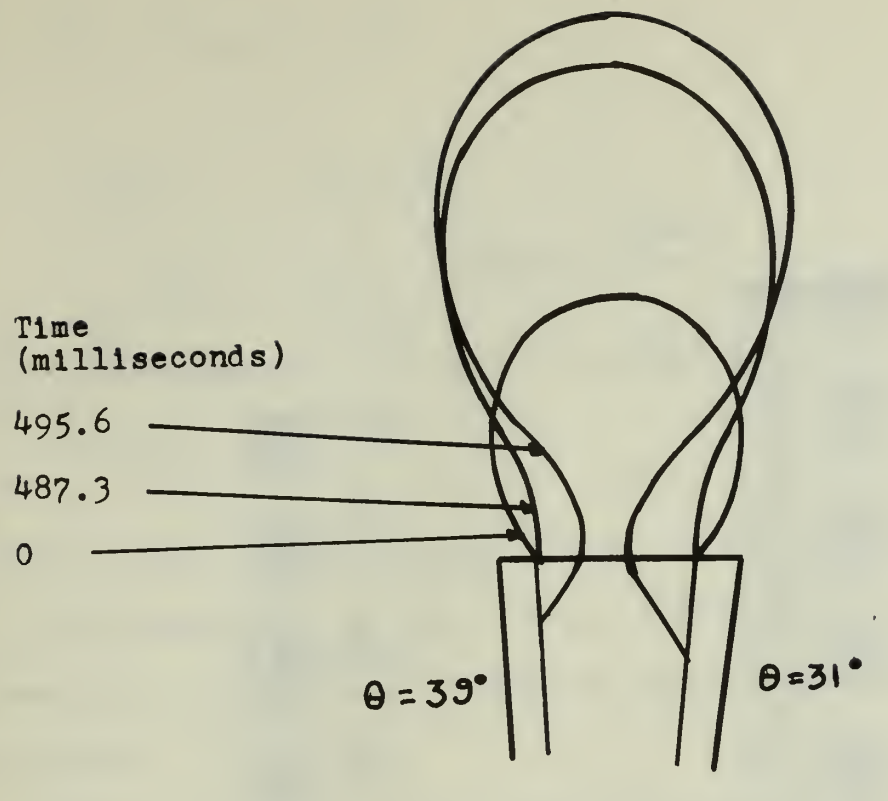

FIG. 8(a)

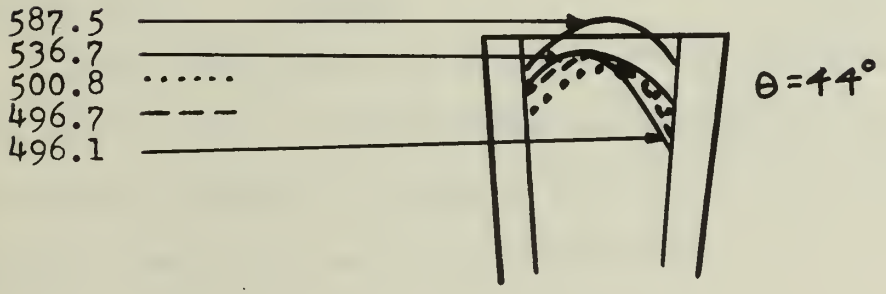

FIG. 8(b)

Bubble and Liquid-Vapor Interface Profiles for Large Conical Cavity in Ethanol

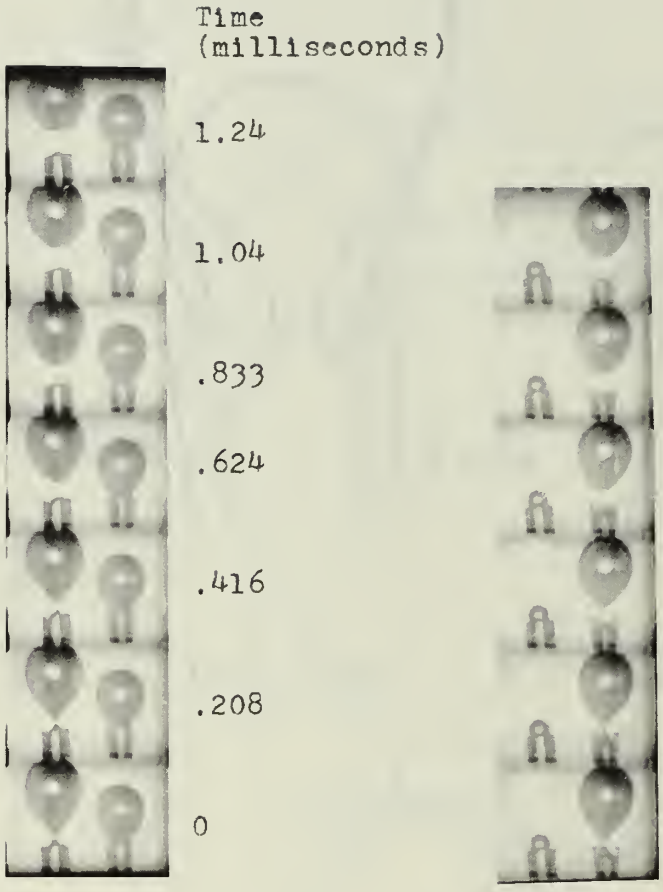

Film Speed 4800 fps

FIG. 9

Photographs of
Bubble Departure and Interface Motion for Cylindrical and Conical Cavities Boiling in Water with Wetting Agent

$$\gamma_{SV} - \gamma_{SL} = \gamma_{LV} \cos \theta \qquad (1)$$

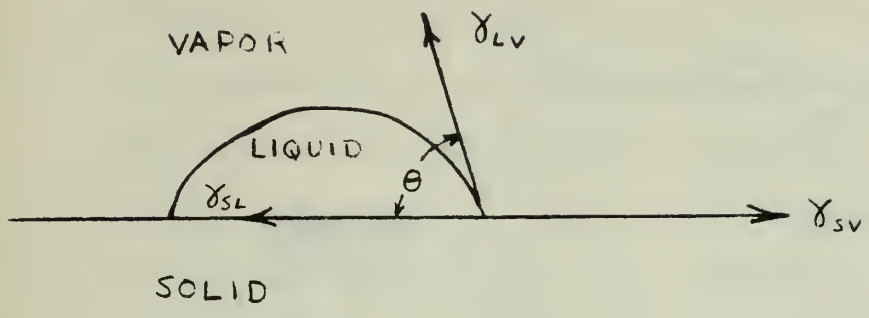

He further states that experimental methods are available to measure γ_{LV} but measurements of γ_{SV} and γ_{SL} are difficult. Therefore, the expected results obtained by addition of the wetting agent to water are uncertain.

Another variable which could certainly account for the decrease in penetration distance of water with wetting agent when compared with water is the cleaning procedure used. Since uncleaned cavities exhibited no interface penetration, then it is conceivable that the cavities used for the water with wetting agent run were slightly contaminated. This is likely since the time to mount the cavities was determined to be a critical factor.

In their theory, Marto and Rohsenow predict that heat flux has a direct effect upon penetration distance. Since it was not certain that heat flux was constant for each run, then this may also have caused the unexpected results for water with wetting agent.

3.1.3 Boiling Water With Sucrose Solution.

Figure 10 shows pictures of cylindrical and conical cavities boiling simultaneously in a water with sucrose solution. Notice that for each cavity, the interface penetration is already at the maximum penetration distance after bubble departure. Again the slight interface motion is

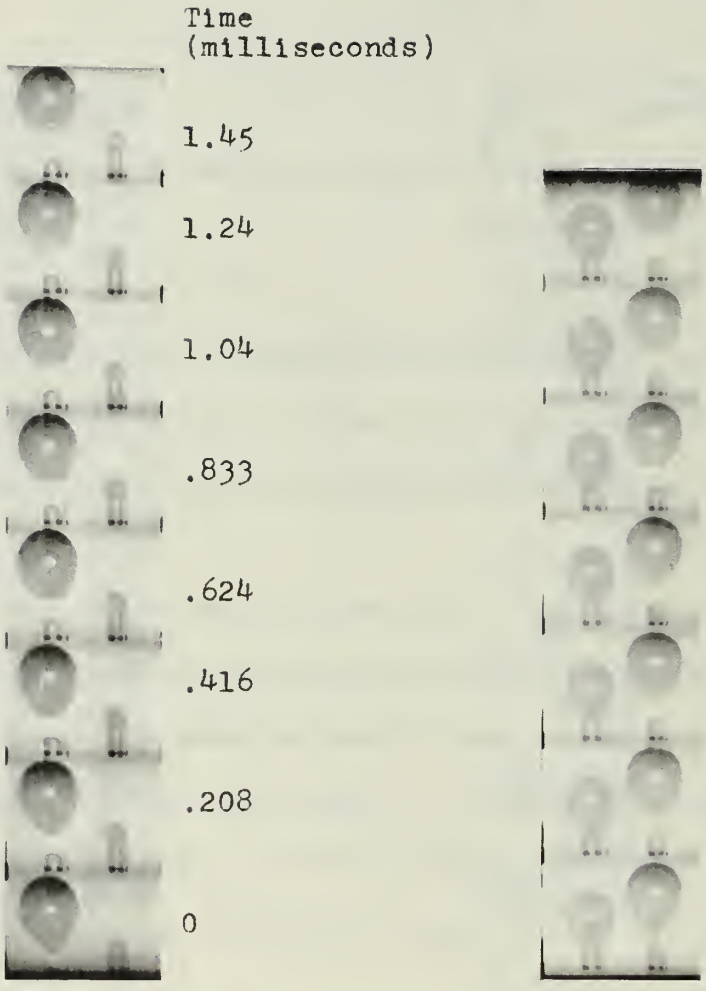

Film Speed 4800 fps

FIG. 10

Photographs of
Bubble Departure and Interface Motion for Cylindrical and Conical Cavities Boiling in Water with Sucrose

due to the tendency for the interface to become symmetrical. Figure 7 shows the bubble necking down and the interface penetration after bubble departure. The contact angle here is slightly greater than that for water indicating that the fluid wets the surface to a lesser extent than water. Table III shows the effect of a viscous fluid on penetration distance. The values of x* are less in the sucrose solution than for the same cavities in water. Again the effect of radius of curvature on penetration distance is demonstrated when a comparison of x* for the conical and cylindrical cavity is made.

3.1.4 Boiling Ethanol.

As was explained in the section on experimental procedures, the conical and cylindrical cavities deactivated quickly when boiling with ethanol. Figures 11 and 12 show all four cavities boiling in ethanol. In each case the interface penetration is apparent. Notice that the interface penetration is greater in the cylindrical cavity than in the conical. This is shown in the data of Table III. This is contrary to the prediction of Marto and Rohsenow and also contrary to the results mentioned above while boiling with other fluids. A plausible explanation for this discrepancy is that evaporation of the liquid in the bottom of the cavity could distort the liquid-vapor interface at the top of the cavity. This would cause less penetration of the interface. While observing the experimental run of the large conical and cylindrical cavities in ethanol, it was noticed that when the first bubble departed from the conical cavity and before vigorous boiling commenced, the interface penetration was very deep. As a result of the inrush of liquid some of the liquid flowed into the bottom of the cavity. The amount of liquid in the cavity increased until the cavity deactivated. Deactivation occurred

Film Speed 4800 fps

FIG. 11

Photographs of
Bubble Departure and Interface Motion for Cylindrical
and Conical Cavities Boiling in Ethanol

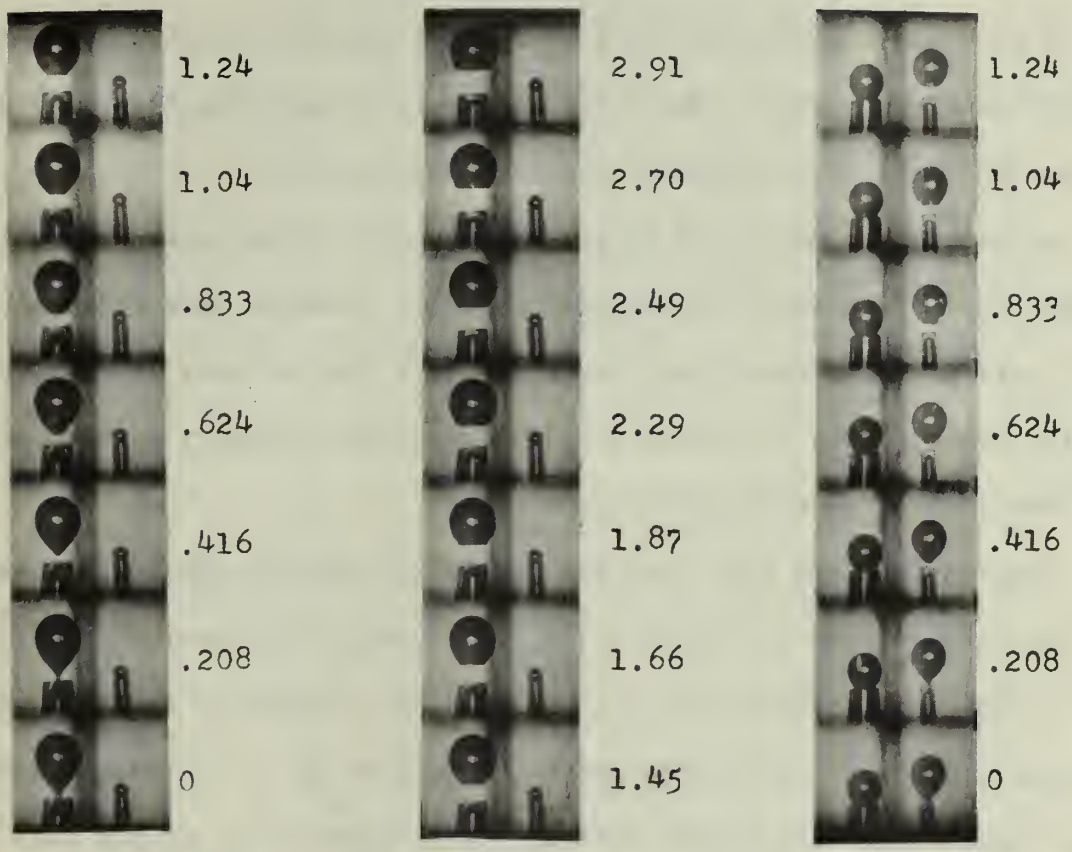

Reentrant Cavity

Small Cylindrical Cavity

FIG. 12

Photographs of
Bubble Departure and Interface Motion for Reentrant and Small Cylindrical Cavities Boiling in Ethanol

approximately fifteen seconds after vigorous boiling began. It was also observed immediately before operation with the camera, that there was only a very small amount of fluid in the cylindrical cavities but none in the reentrant cavity. Therefore, it appears that this interface distortion would be most apparent in the conical cavity.

As previously mentioned in the experimental procedures, the conical and cylindrical cavities deactivated rapidly. However, the reentrant cavity did not deactivate until approximately five minutes after vigorous boiling began. This indicates that the reentrant geometry is more stable than the conical or cylindrical geometries.

Figures 8(a) and 8(b) show the growth and necking down of the bubble and the liquid-vapor interface after departure for the conical cavity. Notice that the interface contact angle is much less than that for water. The deep interface penetration and the reduction of the interface contact angle demonstrates the better wetting characteristics of fluids with reduced surface tension. These two factors also increase the likelihood of cavity deactivation by fluid flow down the cavity walls which was observed in the runs with ethanol.

3.2 Bubble Growth and Departure.

Figures 13 and 14 are growth curves for all four cavity geometries in water. All curves exhibit the same general shape. The large cylindrical and conical cavities have the same departure diameter, however the large reentrant cavity has a slightly larger departure diameter. This was unexpected since DuBois [4] found that cavity geometry has a small effect upon bubble growth and departure diameter. This difference was probably due to the manner in which the bubbles departed from the cylindrical and conical cavities. As shown previously in Fig. 5(a) the bubble departing

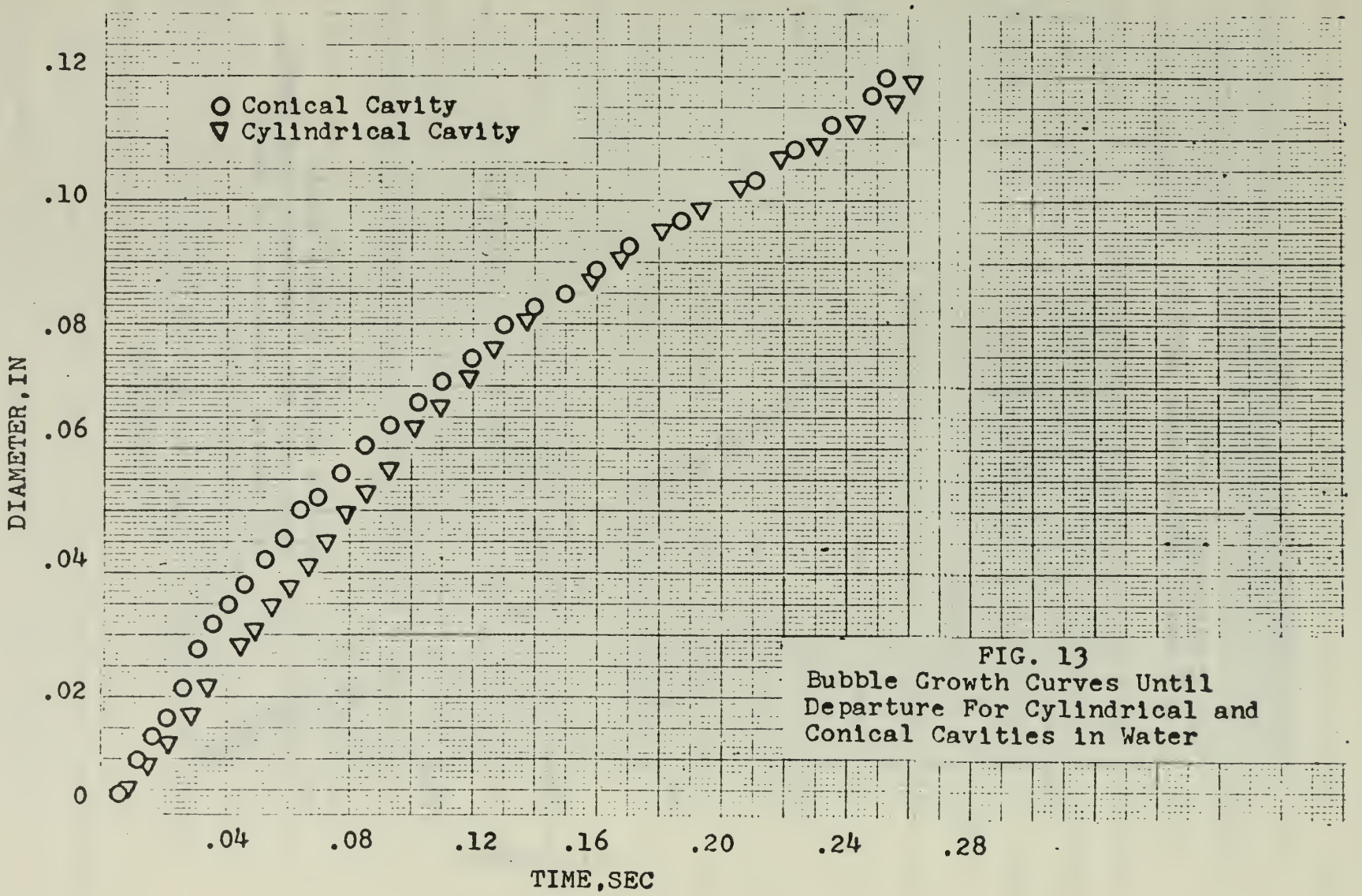

FIG. 13
Bubble Growth Curves Until Departure For Cylindrical and Conical Cavities in Water

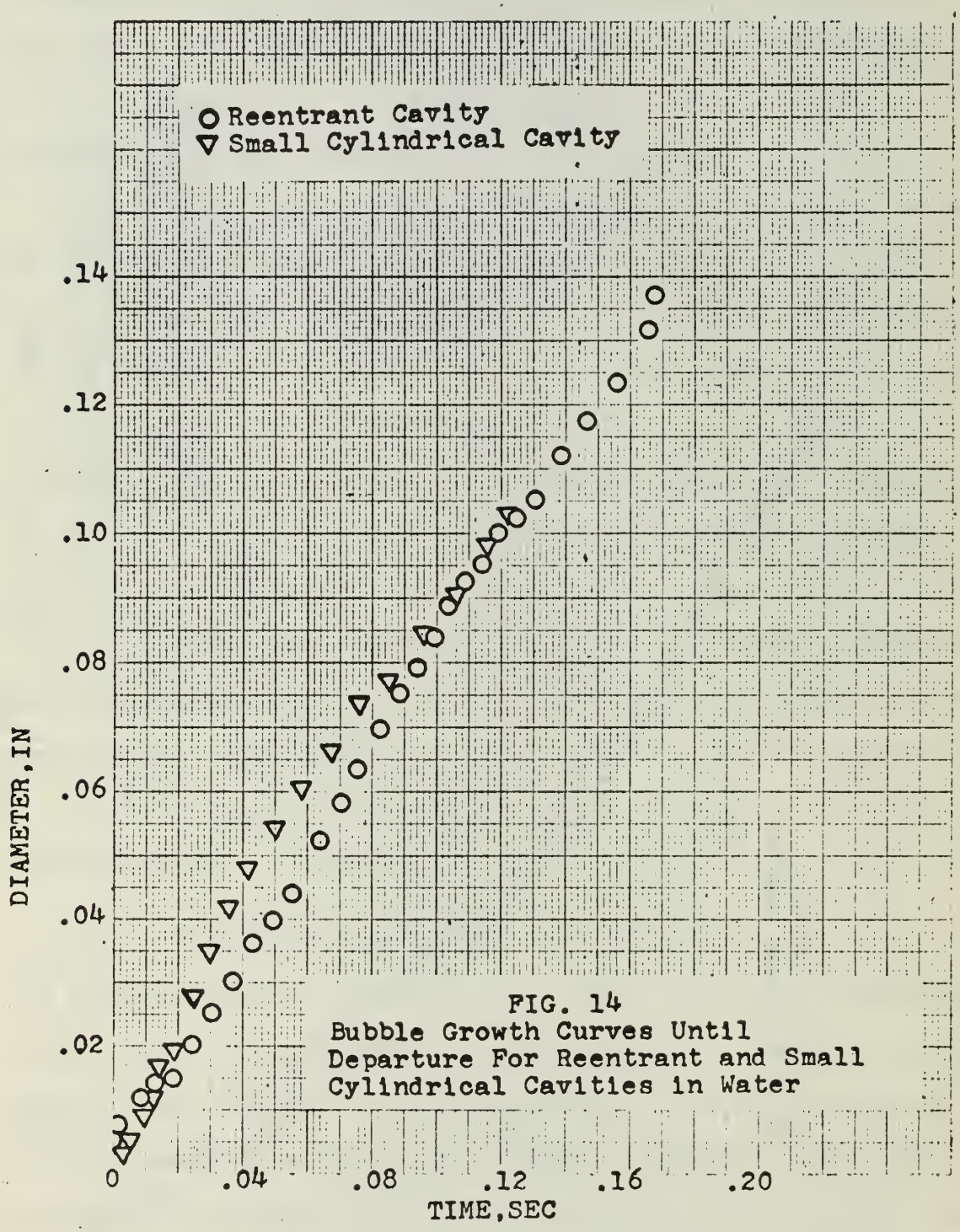

FIG. 14
Bubble Growth Curves Until Departure For Reentrant and Small Cylindrical Cavities in Water

from the conical cavity is skewed to one side. The cylindrical cavity also exhibited this asymmetrical necking down to a lesser extent. This may have caused premature breakoff of the stem of the bubble resulting in a smaller departure diameter. The small cylindrical cavity exhibits a smaller departure diameter but a faster growth time than the large cylindrical cavity. This finding agrees with the well known trend that the product of frequency, f, and diameter, D, is constant. The difference in departure diameters for the large and small cylindrical cavities shows that cavity inner diameter has a direct effect upon departure diameter.

Figure 15 shows the bubble growth curves for the large conical and cylindrical cavities in water with wetting agent. The curves are similar in shape and the cavities exhibit approximately the same departure diameters. The departure diameters for these two cavities are slightly less than those for the same cavities in water. This was expected since Fritz [7] and Staniszewski [8] predict that the departure diameter is proprotional to $\sqrt{\sigma}$.

For water with wetting agent, at 212°F, σ is decreased from 58.9 dynes/cm (for pure water) to 26.2 dynes/cm. It was expected that the growth time in water with wetting agent would be less than the growth time in water due to the decreased surface tension. This was the case as can be seen by a comparison of Figs. 13 and 15. However, it is not certain that the heat input to the boiler was the same for the runs of Figs. 13 and 15 due to the method of heating used. The effect of the surface tension on growth will be discussed further when considering bubble growth in ethanol.

Figure 16 shows the growth curves for the large conical and cylindrical cavities in a water with sucrose solution. When compared with the

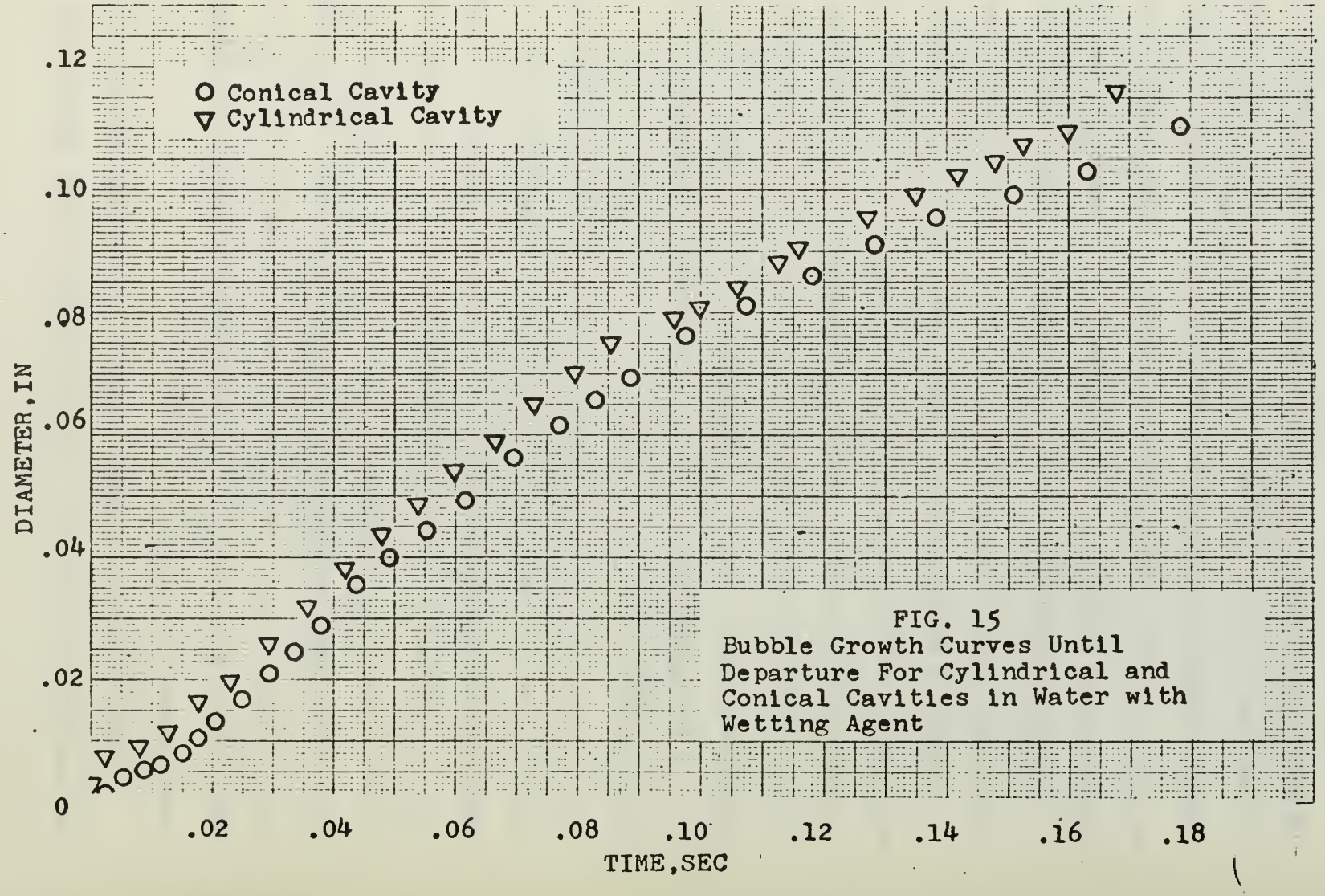

FIG. 15
Bubble Growth Curves Until Departure For Cylindrical and Conical Cavities in Water with Wetting Agent

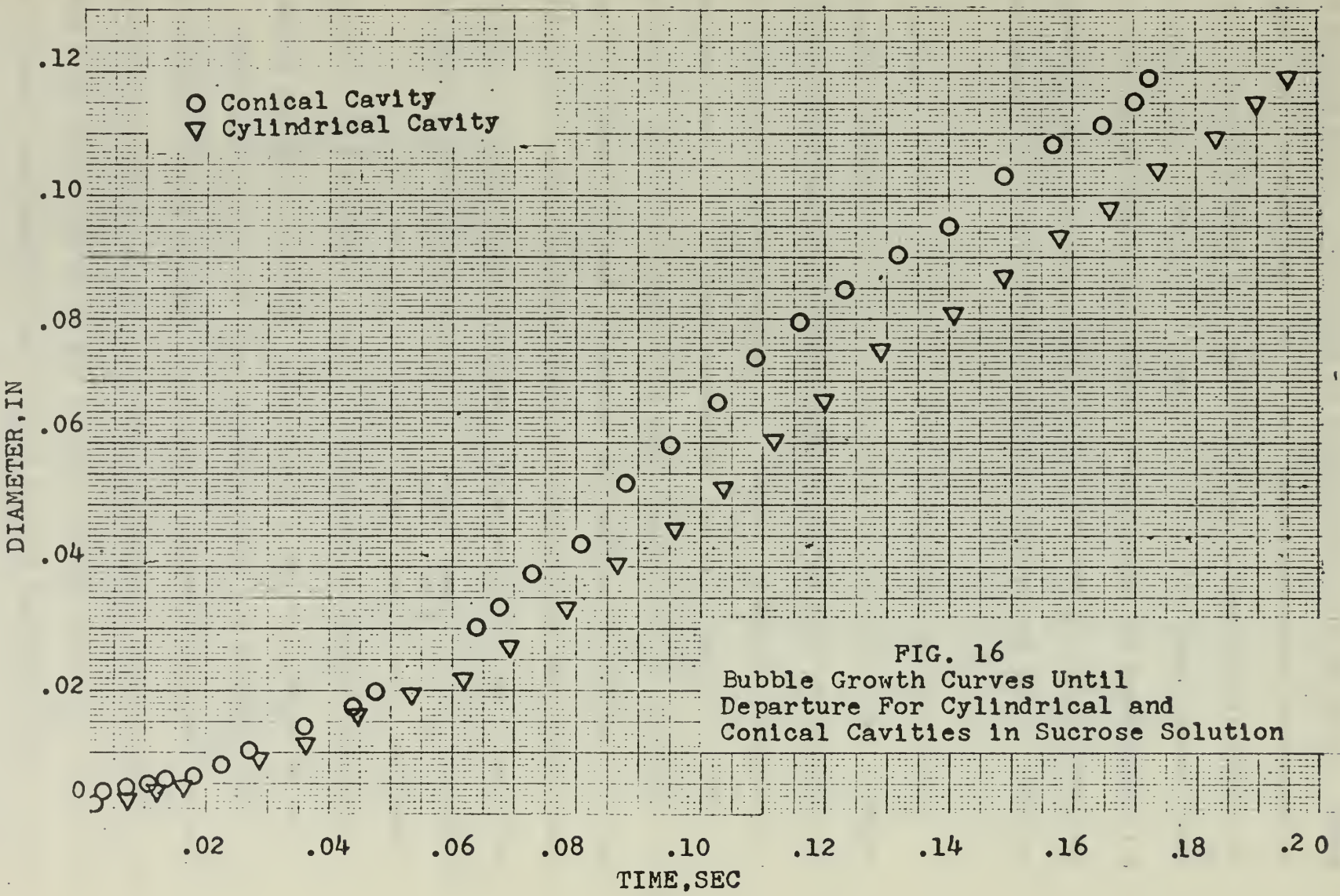

FIG. 16
Bubble Growth Curves Until Departure For Cylindrical and Conical Cavities in Sucrose Solution

growth curves for the same cavities in water, Fig. 13, it is seen that the departure diameters are essentially the same; however, the shape of the curves is different. The effect of a more viscous fluid is seen to delay bubble growth at the initial stages of growth. However, the overall growth times for the cavities in the sucrose mixture are less than the growth times for the same cavities in water. This was unexpected but again it was not certain if the heat input to the boiler was constant for both of these runs.

Figures 17 and 18 are curves for all four cavities in ethanol. The departure diameters are in all cases less than the departure diameters for the same cavities in water. This again was expected due to the reduced surface tension of ethanol. The growth time for the large cylindrical cavity is longer than for the conical cavity. With the same departure diameters, it would appear that the growth times would be the same since the product fD is predicted constant. However, DuBois [4] has shown in his work that individual bubbles from one cavity may follow different curves, (i.e., have different departure times) but the curves essentially have the same shape. This variation in growth curves is probably due to eddying effects of heat within the boiler.

As has been mentioned earlier, it was not certain that heat input to the boiler was constant for all runs. This fact alone was enough to vary bubble growth and thus departure time from one run to another. The effects of surface tension and viscosity on bubble growth therefore would not correlate when comparing any two runs. In an attempt to determine the effect of reduced surface tension and increased viscosity on growth rate, a non-dimensional plot of bubble diameter/departure diameter vs. time/departure time was drawn, (see Fig. 19). Notice that the curve for the sucrose solution is significantly lower than the curve for water in

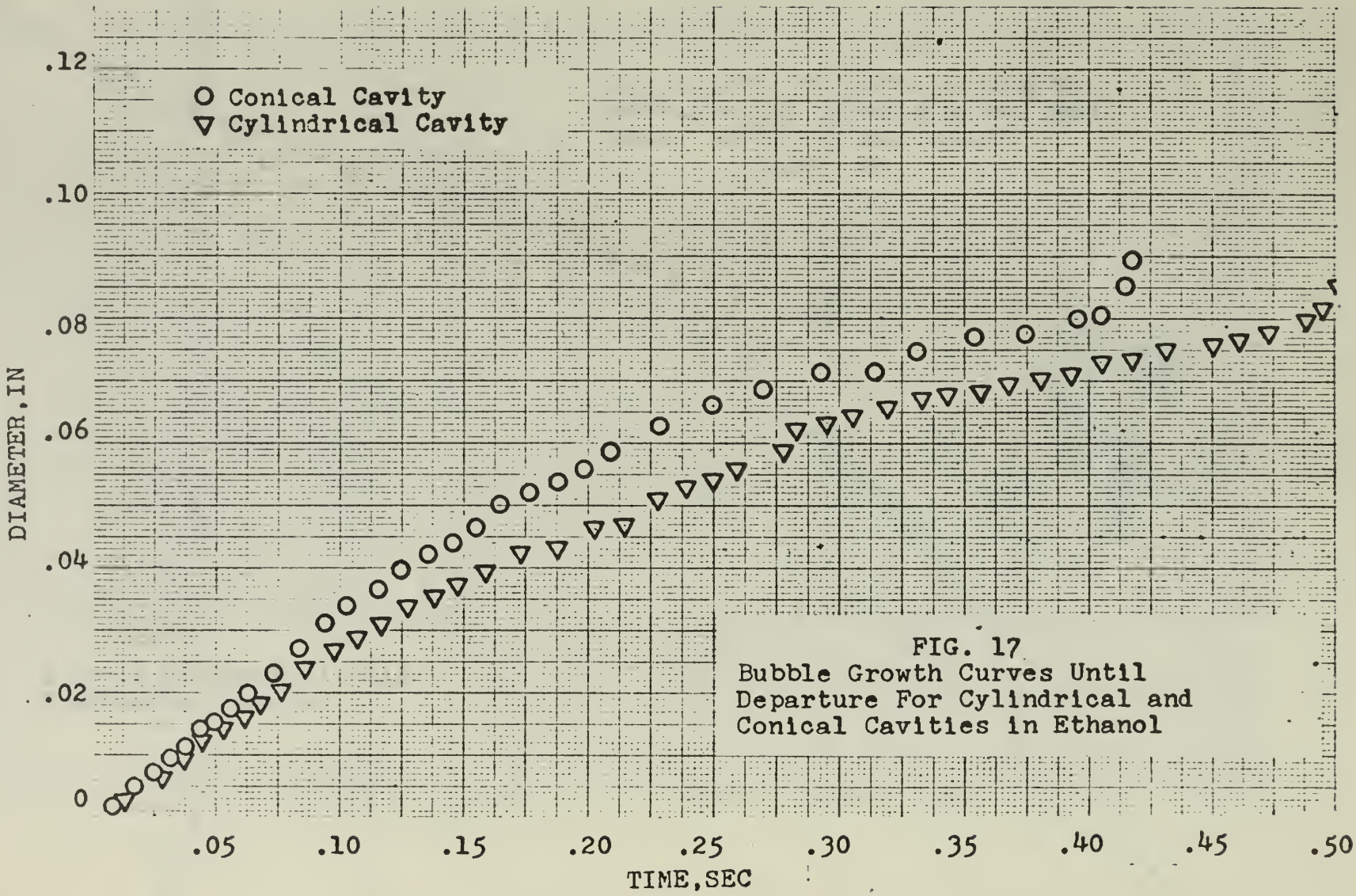

FIG. 17
Bubble Growth Curves Until Departure For Cylindrical and Conical Cavities in Ethanol

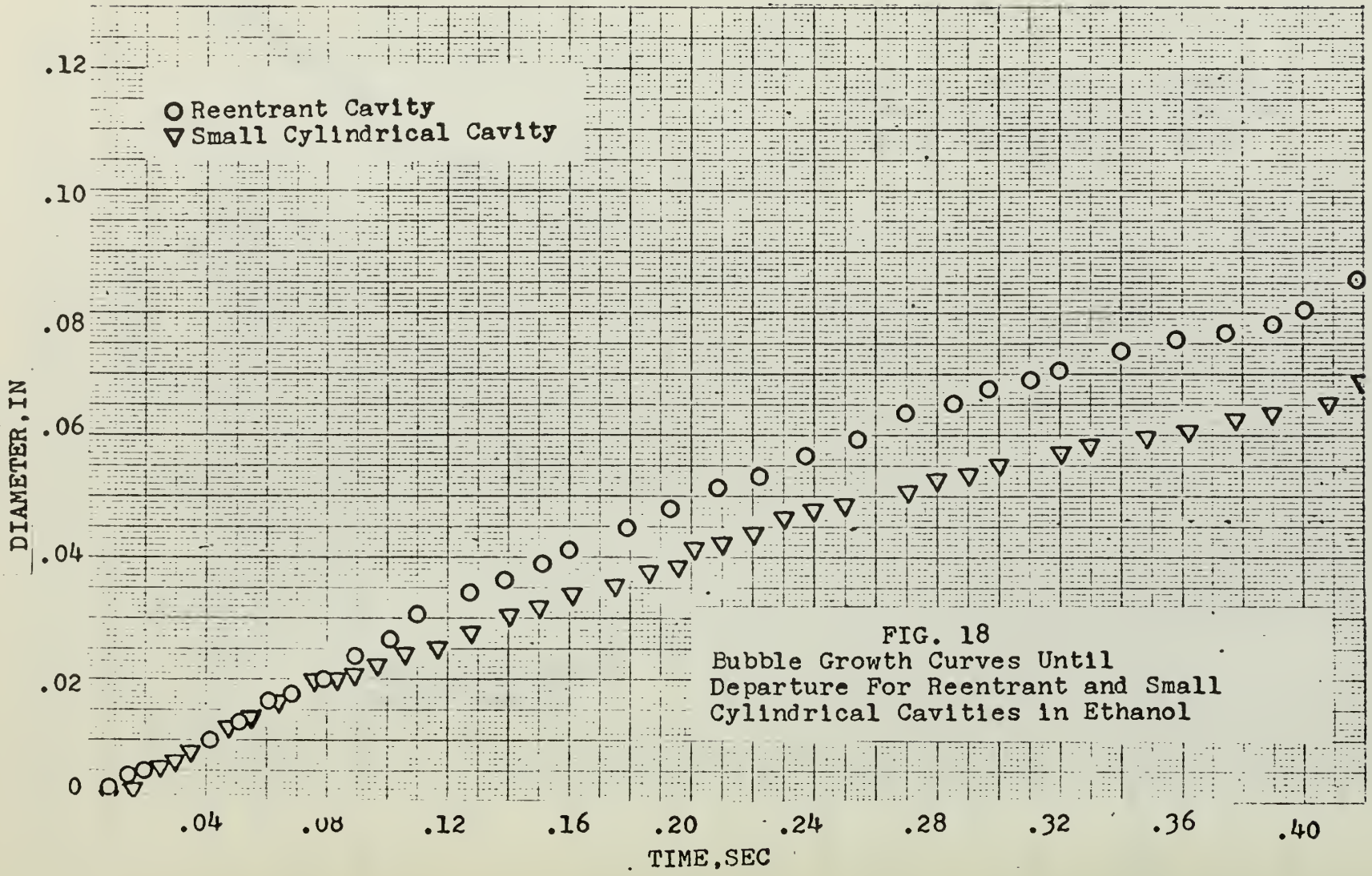

FIG. 18
Bubble Growth Curves Until Departure For Reentrant and Small Cylindrical Cavities in Ethanol

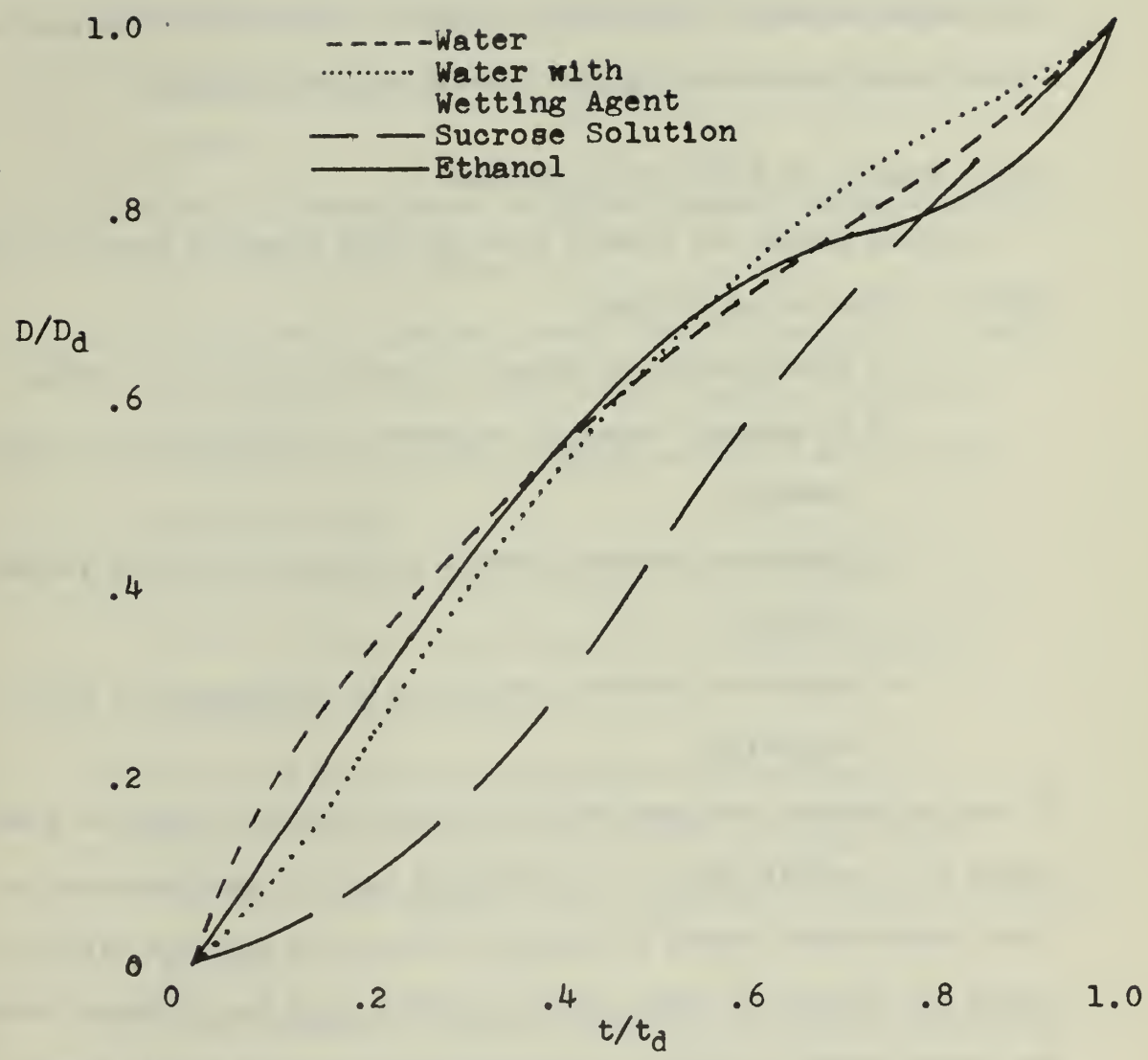

FIG. 19

Nondimensional Plot of Bubble Diameter/Departure Diameter vs. Time/Departure Time For Conical Cavity in Various Fluids.

the early stages of growth. It was expected that bubbles in fluids with reduced surface tension would have faster growth rates. However, Fig. 19 shows that the curves for water with wetting agent and ethanol are similar to water. Therefore it appears that surface tension had little effect upon bubble growth rate during these tests.

3.2.1 Summary of Bubble Growth Curves.

Certain trends are evident from the data presented here for various fluids. These are as follows:

1) Bubble departure diameter depends upon cavity radius.
2) In general, departure diameter is independent of cavity geometry.
3) Departure diameter appears to depend upon fluid surface tension.
4) Departure diameter appears to be independent of fluid viscosity.

It must be pointed out that these are trends observed based on growth curves for a single bubble. As mentioned earlier, perturbations in local temperatures caused by irregular convection currents within the boiler may affect the growth time and growth rate for different bubbles. The growth curves presented here demonstrate typical bubble growth. However, the results of many bubbles for a given fluid should be averaged to obtain a better understanding of the effects of surface tension and viscosity on growth rate and bubble departure diameter.

4. CONCLUSIONS

The following conclusions are arrived at on the basis of experimental evidence:

1) For the sizes of cavities used in this experimental work, nucleate boiling cannot be sustained when boiling with ethanol.
2) Inertia forces appear to be the dominant factor in liquid-vapor interface motion.
3) Liquid-vapor interface penetration decreases as the radius of curvature of the liquid-vapor interface increases.
4) Liquid-vapor interface penetration decreases as cavity radius decreases.
5) Interior cleanliness of the glass model capillary has a direct influence upon wettability and upon interface penetration distance.
6) Viscosity reduces interface penetration distance.
7) Bubble departure diameter increases as cavity radius increases, but appears to be independent of cavity internal geometry.
8) Bubble departure diameter depends upon surface tension but is independent of viscosity.
9) Bubble growth curves appear independent of surface tension.
10) Bubble growth in viscous fluids is retarded during the initial stages of growth.

5. RECOMMENDATIONS FOR FUTURE WORK

The following work is recommended in an effort to better understand the variables affecting nucleate boiling:

1) Improve capillary cleaning methods in order that three cavities may be boiled simultaneously to obtain reproducible results.
2) Determine the effect of variation in heat flux and capillary temperature profile on penetration distance.
3) Determine the effects of pressure and gravity on penetration distance.
4) Boil with fluids of large density differences to determine the effect of inertia forces on the boiling mechanism.
5) Conduct further study of the effect of surface tension on boiling.
6) Boil with artificial cavities of various lengths but constant inside diameter to observe effect of depth on cavity stability.

BIBLIOGRAPHY

1. Rohsenow, W. M., Editor, "Developments in Heat Transfer", Massachusetts Institute of Technology Press, 1964, pp. 177-190.

2. Westwater, J. W., "Boiling Heat Transfer", American Scientist, 47, 1959, pp. 427-445.

3. Marto, P. J., W. M. Rohsenow, "Nucleate Boiling Instability of Alkali Metals, " J. Heat Transfer, 88, Series C, May 1966, pp. 183-195.

4. DuBois, D. R., "Photographic Investigation of Bubble Nucleation from Glass Capillary Tubes". M.S. Thesis, Naval Postgraduate School, Monterey, California, 1967.

5. Zisman, W. A., "Relation of Chemical Constitution to the Wetting and Spreading of Liquids on Solids", Presented at Office of Naval Research Dicennial Symposium, Washington, D. C., March 19, 1957.

6. Fritz, W., "Berechnung Des Maxmal Volumens Von Dampfblasen," Physikalische Zeitschrift, 36, Jan., 1935.

7. Staniszewski, B. E., "Nucleate Bubble Growth and Departure," MIT Report #DSR-7673, Aug. 1959.

INITIAL DISTRIBUTION LIST

		No. Copies
1.	Defense Documentation Center Cameron Station Alexandria, Virginia 22314	20
2.	Library Naval Postgraduate School Monterey, Calif. 93940	2
3.	Mechanical Engineering Department Naval Postgraduate School Monterey, Calif. 93940	2
4.	Prof. P. J. Marto Mechanical Engineering Department Naval Postgraduate School Monterey, Calif. 93940	3
5.	Naval Ship Systems Command (Code 2052) Navy Department Washington, D. C. 20360	1
6.	LT J. C. Eller, USN Engineering Department U. S. Naval Academy Annapolis, Md. 21402	2

DOCUMENT CONTROL DATA - R & D

(Security classification of title, body of abstract and indexing annotation must be entered when the overall report is classified)

1. ORIGINATING ACTIVITY *(Corporate author)*
Naval Postgraduate School
Monterey, California 93940

2a. REPORT SECURITY CLASSIFICATION
Unclassified

2b. GROUP

3. REPORT TITLE
A Photographic Investigation of Bubble Nucleation From Artificial Cavities

4. DESCRIPTIVE NOTES *(Type of report and inclusive dates)*
None

5. AUTHOR(S) *(First name, middle initial, last name)*
Eller, John Christian

6. REPORT DATE	7a. TOTAL NO. OF PAGES	7b. NO. OF REFS
June 1968	54	7

8a. CONTRACT OR GRANT NO.

b. PROJECT NO.
N/A

c.

d.

9a. ORIGINATOR'S REPORT NUMBER(S)
N/A

9b. OTHER REPORT NO(S) *(Any other numbers that may be assigned this report)*

10. DISTRIBUTION STATEMENT
[redacted]

11. SUPPLEMENTARY NOTES
DOWNGRADED
APPROVED FOR PUBLIC RELEASE
[redacted]

12. SPONSORING MILITARY ACTIVITY
Naval Postgraduate School
Monterey, California 93940

13. ABSTRACT

High speed motion pictures of bubble nucleation from glass capillaries were obtained. The fluids used were: distilled water, water with wetting agent, water with sucrose, and ethanol. Capillaries of cylindrical, conical, and reentrant geometries were used with inner diameters ranging from .0182 to .0381 inches.

The penetration of the liquid-vapor interface into a cavity after bubble departure appeared to be inertia controlled. Cavity interior geometry and cleanliness had a direct effect upon the liquid-vapor interface penetration distance. The depth of penetration of the interface increased as cavity size increased. Viscosity reduced the interface penetration.

Bubble growth curves were obtained for a typical bubble in each fluid. Bubble departure diameter appeared to be independent of cavity geometry but increased as cavity size increased. Viscosity retarded bubble growth during the initial stages of growth.

14 KEY WORDS	LINK A		LINK B		LINK C	
	ROLE	WT	ROLE	WT	ROLE	WT
High Speed Photography						
Glass Capillaries						
Artificial Cavities						
Bubble Nucleation						
Bubble Growth and Departure						